ISSN 1672-9145 **Acta Biochimica et Biophysica Sinica** 2005, **37**(9): 613–617 **CN** 31-1940/Q

Expression, Purification and Crystal Structure of a Truncated Acylpeptide Hydrolase from *Aeropyrum pernix* K1

Hai-Feng ZHANG, Bai-Song ZHENG[1], Ying PENG, Zhi-Yong LOU, Yan FENG[1]*, and Zi-He RAO*

Laboratory of Structural Biology, Department of Biological Sciences and Biotechnology and Protein Sciences Laboratory of Ministry of Education, Tsinghua University, Beijing 100084, China;
[1] *Key Laboratory for Molecular Enzymology and Engineering of Ministry of Education, Jilin University, Changchun 130023, China*

Abstract Acylpeptide hydrolase (APH) catalyzes the N-terminal hydrolysis of N^{α}-acylpeptides to release N^{α}-acylated amino acids. The crystal structure of recombinant APH from the thermophilic archaeon *Aeropyrum pernix* K1 (apAPH) was reported recently to be at a resolution of 2.1 Å using X-ray diffraction. A truncated mutant of apAPH that lacks the first short α-helix at the N-terminal, apAPH-Δ(1-21), was cloned, expressed, characterized and crystallized. Data from biochemical experiments indicate that the optimum temperature of apAPH is decreased by 15 °C with the deletion of the N-terminal α-helix. However, the enzyme activity at the optimal temperature does not change. It suggests that this N-terminal α-helix is essential for thermostability. Here, the crystal structure of apAPH-Δ(1-21) has been determined by molecular replacement to 2.5 Å. A comparison between the two structures suggests a difference in thermostability, and it can be concluded that by adding or deleting a linking structure (located over different domains), the stability or even the activity of an enzyme can be modified.

Key words acylpeptide hydrolase; *Aeropyrum pernix* K1; crystal structure

Acylpeptide hydrolase (APH; also known as acylamino acid-releasing enzyme or acylaminoacyl peptidase [EC3.4.19.1]), a member of the prolyl oligopeptidase (POP) family of serine proteases, catalyzes the N-terminal hydrolysis of N^{α}-acylpeptides to release N^{α}-acylated amino acids [1]. In addition to APH, the members of the prolyl oligopeptidase family include dipeptidyl peptidase IV (DPP IV), fibroblast activation protein α, DPP7, DPP8, DPP9, prolyl carboxypeptidase, oligopeptidase B and prolyl oligopeptidase. Most of them are important in the research for new drugs [2,3].

To date, rat, porcine, human and bovine APH from various tissues have been characterized. They all consist of 732 amino acid residues, and were reported to form homotetramers [4–8]. However, *Arabidopsis thaliana* APH is a 764-amino acid protein, which exhibits 31.8% sequence identity with rat APH, and it also forms a tetramer [9]. An APH from the thermophilic archaeon *Pyrococcus horikoshii* OT3 has also been characterized. Being different from its mammalian counterparts, it is 100 residues shorter and forms a homodimer [10]. Inhibition of APH activity leads to apoptosis [11], and a deficiency in human APH is reported to be linked to small-cell lung carcinoma and renal cell carcinoma [12–14]. APH in the porcine brain may be the target of the cognitive-enhancing effects of certain organophosphorus compounds [15].

Like *P. horikoshii* OT3, *Aeropyrum pernix* K1 grows in the temperature range of 90 to 98 °C, with an optimal temperature of 95 °C. However, *P. horikoshii* OT3 is an anaerobic euryarchaeota, and *A. pernix* K1 is an aerobic strain classified as crenarchaeota. The complete genome of *A. pernix* K1 has been sequenced, and four genes (*Ape*1547, *Ape*1832, *Ape*2290 and *Ape*2441) have been designated as encoding APHs [16]. Recently, the crystal structure of an APH from *A. pernix* K1 (apAPH), the gene product of *Ape*1547, was determined [17]. This is the first confirmed structure of an APH. Formerly, only human

Received: March 20, 2005 Accepted: June 7, 2005
*Corresponding authors:
Yan FENG: Tel, 86-431-8987975; E-mail, yfeng@jlu.edu.cn
Zi-He RAO: Tel, 86-10-62771493; Fax, 86-10-62773145; E-mail, raozh@xtal.tsinghua.edu.cn

DOI: 10.1111/j.1745-7270.2005.00085.x

APH has been crystallized, but the structure remains unknown [18].

apAPH is a symmetric homodimer, and each monomer comprises two domains. The N-terminal domain is a seven-bladed β-propeller and the C-terminal catalytic domain has a canonical α/β hydrolase fold [17]. A short α-helix at the N-terminus (residues 8–23) extends from the β-propeller domain and forms part of the hydrolase domain; this forms a linking structure between these two domains.

To investigate how this N-terminal α-helix affects the whole structure, enzyme activity and thermostability, a mutant of apAPH in which the first 21 amino acids at the N-terminus were removed, apAPH-Δ(1-21), was expressed in *Escherichia coli*, and its crystal structure was determined.

Materials and Methods

Materials

The expression vector pET11a-apAPH-Δ(1-21) was constructed by the Key Laboratory of Molecular Enzymology and Engineering of Ministry of Education, Jilin University (Changchun, China). The *E. coli* BL21(DE3) strain was obtained from Novagen (Darmstadt, Germany, and chromatography columns were purchased from Amersham Pharmacia Biotech (Uppsala, Sweden). General reagents were of analytical grade.

Protein expression and purification

The expression vector pET11a-apAPH-Δ(1-21) was transformed into the *E. coli* BL21(DE3) strain. The conditions for expression were as follows. Bacteria were grown in LB medium (10 mg/ml tryptone, 5 mg/ml yeast extract, 10 mg/ml NaCl) containing 100 μg/ml penicillin at 37 °C until A_{600}=0.6, then induced with 0.5 mM isopropyl-β-*D*-thiogalactopyranoside (IPTG). After treatment at 25 °C overnight, the cells were harvested by centrifugation at 5000 rpm for 10 min, resuspended in 25 mM Tris-HCl (pH 8.0) and 50 mM NaCl, and lysed by sonication. The soluble cell lysate obtained by centrifugation at 15,000 rpm for 30 min was heated at 75 °C for 1 h. Then the supernatant obtained by centrifugation was loaded onto a Q Sepharose fast flow column previously equilibrated with 25 mM Tris-HCl (pH 8.0) containing 50 mM NaCl. After washing away the unbound protein with two bed volumes of 25 mM Tris-HCl (pH 8.0), a linear gradient of 0.05–1 M NaCl in the same buffer was applied. The collected fractions were centrifuged for 30 min at 15,000 rpm. The supernatant was then loaded onto a Resource Q anion-exchange chromatography column equilibrated with 25 mM Tris-HCl (pH 8.0) containing 50 mM NaCl. The eluted sample was concentrated using Filtron 5K to 250 μl and loaded onto a Superdex 75 size-exclusion chromatography column. The fraction showing only one protein band with a molecular weight of about 60 kDa after SDS-PAGE was collected and its purity was determined to be suitable for crystallization.

Crystallization

The purified protein was concentrated using Filtron 5K to 25 mg/ml in a solution containing 50 mM NaCl. apAPH crystallization conditions were used for the initial screening using the hanging-drop vapor diffusion method. The mixed drop including 1.5 μl of protein solution and 1.5 μl of reservoir solution was grown in an airtight system containing 0.4 ml of reservoir solution at 18 °C. Crystals appeared after one month with the protein concentration higher than 25 mg/ml. The best crystallization results were obtained with 4.5%–5% (*W*/*V*) PEG 4000, 0.025 M sodium acetate, pH 4.6. To improve the quality of the crystals, 0.025%–0.05% agarose gel was added.

Data collection and processing

The data were collected to 2.5 Å using a 345 mm MAR research image-plate system mounted on a Rigaku RU-2000 Cu K_α rotating-anode generator (Norderstedt, Germany) operated at 48 kV and 98 mA. During data collection, the crystal was maintained at 100 K using a Cryostream (Oxford Cryosystems, Oxford, UK) in a cryoprotectant prepared by adding 20% glycerol to the mother liquor. The data were processed and scaled with DENZO and SCALEPACK.

Results

Structure determination and refinement

The asymmetric unit of the crystal contains two molecules (denoted A and B) with an approximate solvent content of 44%. The structure of apAPH-Δ(1-21) was determined by molecular replacement with the program AMoRe, using the known structure of apAPH (PDB code 1VE6) as a search model. The program O was used for viewing electron density maps and manual building. Crystallography & NMR system (CNS) was used for refinement, with iterative cycles of simulated annealing and individual B-factor refinement in the resolution range

of 50–2.5 Å. The final structure had R_{work}=22.9% (R_{free}=24.8%), and consisted of 561 residues in molecule A and molecule B respectively and 579 water molecules. From the Ramachandran plot generated by PROCHECK, the final structure was found to have good stereochemistry, with 73.8% of residues in the most favored region, 26% of residues in the additionally allowed region and 0.2% of residues in the generously allowed region. The final refinement statistics for the model are given in **Table 1**.

Comparison with apAPH

Enzymatic assay data indicate that the optimum temperature of apAPH is decreased by 15 °C (from 90 °C to 75 °C) with the deletion of the N-terminal α-helix, but the enzyme activity at the optimal temperature does not change (data not shown). It suggests that this α-helix is essential for thermostability. **Fig. 1** shows the superposition of the C^{α} backbones of apAPH-Δ(1-21) and wild-type apAPH. The main-chain conformations of them are very similar, except for the α-helix at the N-terminus. The root mean square (r.m.s.) deviation of all the main-chain atoms (calculated against molecule A) between the two structures is 0.873 Å. When the two domains are calculated separately, the r.m.s. deviations are 0.801 Å for the N-terminal domain and 0.829 Å for the C-terminal domain. It can be inferred that there are further differences between the C-terminal catalytic domains of two structures.

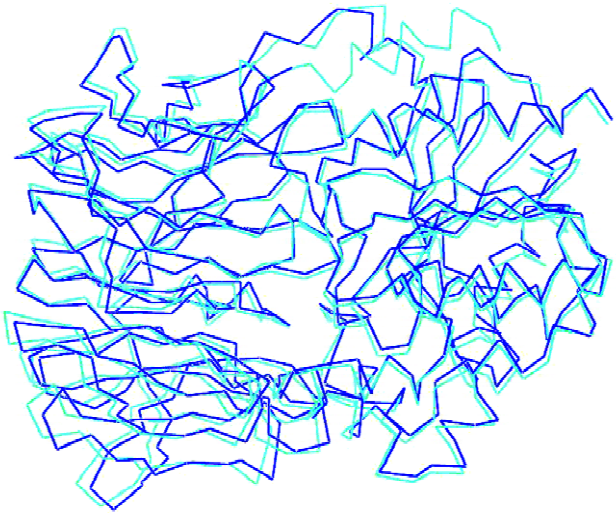

Fig. 1 Superposition of the C^{α} backbones of apAPH-Δ(1-21) (dark blue) and wild-type apAPH (light blue)

Table 1 Data set and refinement statistics

Parameter	Value
Space group	$P2_12_12_1$
Unit cell parameter	
a	63.1 (Å)
b	102.3 (Å)
c	163.9 (Å)
Resolution range	50–2.5 (Å)
Data redundancy	3.8 (3.0)
Completeness	92.6% (91.4%)
$I/\sigma(I)$	8.9 (1.8)
Solvent content	44%
R_{merge}	15.5% (48.7%)
R_{work}	22.9%
R_{free}	24.8%
Residue number	1122
Water molecular number	579
Ramachandran plot	
Most favored regions	73.8%
Additionally allowed regions	26.0%
Generously allowed regions	0.2%
Disallowed regions	0.0%
r.m.s. bond length	0.008 (Å)
r.m.s. bond angle	1.6 (Å)
Average B factors (Å^2)	32.5 (Å^2)

Values in parentheses correspond to the highest resolution shell, 2.59–2.50 Å. r.m.s., root mean square.

The structure of apAPH-Δ(1-21) is more flexible. The average B-factor values are 32.5 Å^2 for apAPH-Δ(1-21) and 19.4 Å^2 for apAPH respectively. It should be noted that the temperature factors are considerably higher for apAPH-Δ(1-21), indicating greater mobility along the polypeptide chain in this structure (**Fig. 2**).

Analysis of the electrostatic surface of apAPH-Δ(1-21) revealed that an additional cavity forms where the N-terminal α-helix existed (**Fig. 3**). It is believed that the cavity in the electrostatic surface is a disadvantage for protein stability.

Discussion

apAPH is a bifunctional enzyme, acting as both APH and esterase. Esterases have developed into the most widely used classes of enzymes in various industrial processes, including stereospecific hydrolysis, transesterification, ester synthesis and modification of physicochemical properties of triglycerides for fat biosynthesis and other

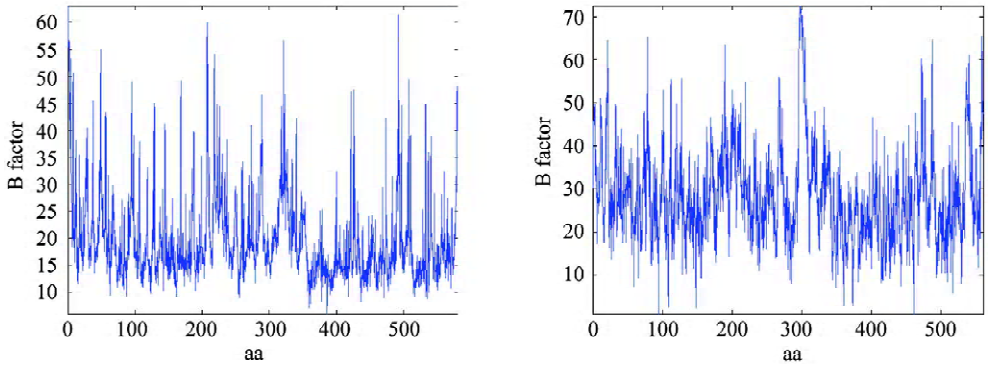

Fig. 2 Mobility along the polypeptide chain given as the average B-factor of atoms of each residue for molecule A

(A) apAPH. (B) apAPH-Δ(1-21).

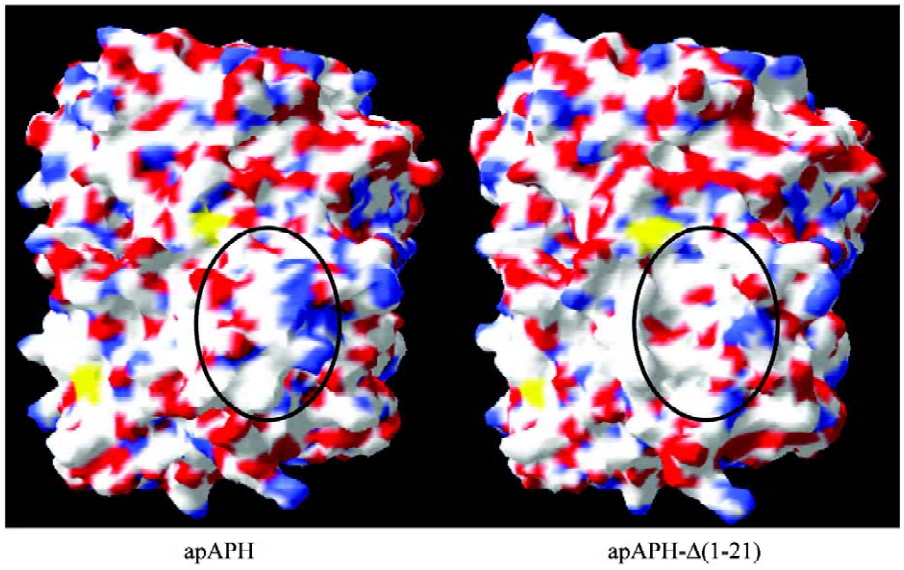

Fig. 3 The electrostatic surface of apAPH and its mutant apAPH-Δ(1-21)

An additional cavity can be found in the mutant. The circled regions represent the cavity.

organic biosynthesis reactions. However, mesophilic enzymes are often not well suited for the harsh reaction conditions, such as high temperature, exposure to organic solvents, etc., in industrial processes because of the lack of enzyme stability. The discovery of a specific esterase able to function under extreme conditions is important and will widely extend the range of reactions in which esterase can be used. Experiments indicate that apAPH has esterase activity in the temperature range of 55 to 95 °C, with maximum activity and highest thermostability at 90 °C (data not shown).

In general, several factors are known to affect the stability of thermophilic proteins. Primary sequence composition, salt bridge/ion pairs and hydrogen bonds, hydrophobic interaction contact area and solvent accessible surface area all contribute to thermostability. In this study, a specific method has been applied and as a result of this, a new method of changing the thermostability of an enzyme to a great extent has been discovered.

In contrast with the percentage of the first 21 amino acids in the total of 582 amino acids (3.6%), the percentages of charged and hydrophobic residues in the truncated sequence are 5.1% and 5.2% respectively. Macroscopically, an increase in the number of charged and hydrophobic residues can enhance thermostability. In addition, there are two important salt bridges (D15-R355

and R18-D325) which also improve the thermal stability. In general, it is believed that a decrease in the solvent-accessible surface area is favorable for protein stability, and the larger cavity results in an increase in solvent accessibility of the structure and thus reduces thermostability. But these values are 20,955 $Å^2$ for apAPH and 20,289 $Å^2$ for apAPH-Δ(1-21). Therefore, the cavity may influence thermostability in other ways.

In conclusion, the decrease in thermostability appears to the result of amino acid composition, fewer ionic interactions and a larger cavity in the structure. Together, these structural features may serve to enhance the thermostability of apAPH. However, as the N-terminal α-helix has no effect on the active site, the enzyme activity of apAPH-Δ(1-21) is the same as that of the wild-type apAPH. Moreover, the structural comparison above suggests that we can change the stability of an enzyme and at the same time retain its activity by adding or deleting a linking structure (located over different domains). A quick modification based on structure is thus possible.

References

1 Tsunasawa S, Narita K, Ogata K. Purification and properties of acylamino acid-releasing enzyme from rat liver. J Biochem (Tokyo) 1975, 77: 89–102

2 Polgar L. The prolyl oligopeptidase family. Cell Mol Life Sci 2002, 59: 349–362

3 Rosenblum JS, Kozarich JW. Prolyl peptidases: A serine protease subfamily with high potential for drug discovery. Curr Opin Chem Biol 2003, 7: 496–504

4 Kobayashi K, Lin LW, Yeadon JE, Klickstein LB, Smith JA. Cloning and sequence analysis of a rat liver cDNA encoding acyl-peptide hydrolase. J Biol Chem 1989, 264: 8892–8899

5 Mitta M, Asada K, Uchimura Y, Kimizuka F, Kato I, Sakiyama F, Tsunasawa S. The primary structure of porcine liver acylamino acid-releasing enzyme deduced from cDNA sequences. J Biochem (Tokyo) 1989, 106: 548–551

6 Miyagi M, Sakiyama F, Kato I, Tsunasawa S. Complete covalent structure of porcine liver acylamino acid-releasing enzyme and identification of its active site serine residue. J Biochem (Tokyo) 1995, 118: 771–779

7 Mitta M, Ohnogi H, Mizutani S, Sakiyama F, Kato I, Tsunasawa S. The nucleotide sequence of human acylamino acid-releasing enzyme. DNA Res 1996, 3: 31–35

8 Sharma KK, Ortwerth BJ. Bovine lens acylpeptide hydrolase. Purification and characterization of a tetrameric enzyme resistant to urea denaturation and proteolytic inactivation. Eur J Biochem 1993, 216: 631–637

9 Yamauchi Y, Ejiri Y, Toyoda Y, Tanaka K. Identification and biochemical characterization of plant acylamino acid-releasing enzyme. J Biochem (Tokyo) 2003, 134: 251–257

10 Ishikawa K, Ishida H, Koyama Y, Kawarabayasi Y, Kawahara J, Matsui E, Matsui I. Acylamino acid-releasing enzyme from the thermophilic archaeon *Pyrococcus horikoshii*. J Biol Chem 1998, 273: 17726–17731

11 Yamaguchi M, Kambayashi D, Toda J, Sano T, Toyoshima S, Hojo H. Acetylleucine chloromethyl ketone, an inhibitor of acylpeptide hydrolase, induces apoptosis of U937 cells. Biochem Biophys Res Commun 1999, 263: 139–142

12 Naylor SL, Marshall A, Hensel C, Martinez PF, Holley B, Sakaguchi AY. The DNF15S2 locus at 3p21 is transcribed in normal lung and small cell lung cancer. Genomics 1989, 4: 355–361

13 Scaloni A, Jones W, Pospischil M, Sassa S, Schneewind O, Popowicz AM, Bossa F *et al*. Deficiency of acylpeptide hydrolase in small-cell lung carcinoma cell lines. J Lab Clin Med 1992, 120: 546–552

14 Erlandsson R, Boldog F, Persson B, Zabarovsky ER, Allikmets RL, Sumegi J, Klein G *et al*. The gene from the short arm of chromosome 3, at D3F15S2, frequently deleted in renal cell carcinoma, encodes acylpeptide hydrolase. Oncogene 1991, 6: 1293–1295

15 Richards PG, Johnson MK, Ray DE. Identification of acylpeptide hydrolase as a sensitive site for reaction with organophosphorus compounds and a potential target for cognitive enhancing drugs. Mol Pharmacol 2000, 58: 577–583

16 Kawarabayasi Y, Hino Y, Horikawa H, Yamazaki S, Haikawa Y, Jin-No K, Takahashi M *et al*. Complete genome sequence of an aerobic hyper-thermophilic crenarchaeon, *Aeropyrum pernix* K1. DNA Res 1999, 6: 83–101, 145–152

17 Bartlam M, Wang G, Yang H, Gao R, Zhao X, Xie G, Cao S *et al*. Crystal structure of an acylpeptide hydrolase/esterase from *Aeropyrum pernix* K1. Structure (Camb) 2004, 12: 1481–1488

18 Feese M, Scaloni A, Jones WM, Manning JM, Remington SJ. Crystallization and preliminary X-ray studies of human erythrocyte acylpeptide hydrolase. J Mol Biol 1993, 233: 546–549

Edited by
Wei-Min GONG